De-bonding Strands as an Anchorage Zone Crack Control Method for Pretensioned Concrete Bulb-tee Bridge Girders

Emre Kizilarslan

Graduate Student, University of Wisconsin, Madison, WI, USA

Pinar Okumus

Assistant Professor, University at Buffalo, NY, USA

Michael Oliva

Emeritus Professor, University of Wisconsin, Madison, WI

Abstract Cracks occurring in the anchorage zones of pre-tensioned bridge girders after de-tensioning are a concern because of the possibility of de-icing salts corroding steel reinforcing bars or strands within concrete. This study assessed the efficacy of strand debonding for crack control by instrumenting and simulating full-scale bridge girders with varying ratios of debonded strands (25%, 38% and 62%). Strand debonding over a distance larger than the transfer length and over a short distance from the girder end was investigated. Although 25% debonding reduced strains, it was not sufficient to eliminate cracks. De-bonding 38% of the strands at the girder ends eliminated cracks causing corrosion concerns. Debonding 62% of strands for a short distance resulted in similar or smaller strains in concrete compared to a girder with no debonding.

1 Introduction

Prestressed or precast concrete bridge girders have been widely used all around the world. Deep wide flange girders, or bulb tee girders, have especially gained popularity due to their large load carrying capacities. In order to satisfy service limit states at long spans, however, these girders are heavily prestressed, which causes cracks at the anchorage zones (ends) of these girders during detensioning of strands. The cracks observed in the anchorage zone are categorized by their shapes and are named as inclined cracks (0.1 mm. (0.004 in.)-0.25 mm. (0.010 in.) wide), horizontal web cracks (0.1 mm. (0.004 in.)-0.25 mm. (0.010 in.) wide), and Y cracks (0.5 mm. (0.02 in.)-1.5 mm. (0.06 in.) wide) as shown on a 72 in. deep girder in Fig.1. These cracks might deteriorate a structure's durability by letting aggressive de-icing salts and water to reach prestressing strands. For girder ends exposed to the environment, Y cracks, due to their large crack widths, may need to be repaired before the girder is used on a bridge by grout or epoxy filling. When girder ends are embedded in concrete diaphragms, repair may not be needed [1].

Fig.1. Types of anchorage zone cracks in a 183 cm deep Wisconsin pre-tensioned girder.

In a previous study [2, 3, 4], different crack control methods, including adding reinforcement, changing strand cutting order, lowering or spreading harped strands, debonding all strands for a short distance from the girder end, and debonding some strands over the anchorage zone, have been investigated. This paper focuses on debonding as it was evaluated to be the most effective control method for all types of girder end cracks.

2 Girder Instrumentation Results

To evaluate the effectiveness of debonding, concrete strains in two 183 cm (72 in. or 72W) deep bulb-tee girders and three 137 cm (54 in. or 54W) deep bulb-tee

girders were monitored at different precast plants during strand detensioning using vibrating wire gages. One of the 183 cm girders and two of the 137 cm girders were redesigned with debonded strands and were otherwise identical to the control girders with no debonding. A full description of the instrumentation and results may be found elsewhere [5, 6]. Selected details of the girders are given in Table 1. All girders had 1.52 cm (0.6 in.) diameter, 1862 MPa (270 ksi) ultimate strength, low-relaxation strands.

	Girder 1	Girder 2	Girder 3	Girder 4	Girder 5
Girder depth-cm	183	183	137	137	137
Lengths of Girders-m	47	47	38	38	38
Total Number of Strands	48	48	42	42	42
Number of Draped Strands	8	6	8	8	8
Number of Debonded Strands	-	12	-	16	26

Table 1. Selected girder details.

Configurations of strands for 183 cm deep girder without and with debonding are shown in Fig. 2. The number of debonded strands in this girder was limited to 25% to comply with the AASHTO LRFD Bridge Design Specifications (BDS) [7] 5.11.4.3.

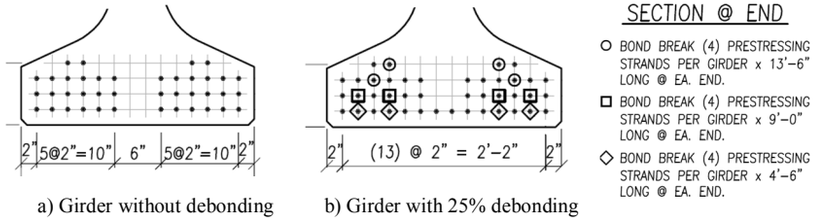

a) Girder without debonding b) Girder with 25% debonding

Fig. 2. Strand patterns for girder end with (a) and without (b) debonded strands.

To measure concrete strain, vibrating wire (VW) gages were embedded in concrete in the Y crack region (VW2, VW3, VW5). Examining the strains in the Y cracking region, debonding created a small difference in concrete strain at the first stirrup (VW2) location but was particularly effective in the third stirrup (VW3) location.

The data from the 183 cm deep girders revealed that 25% strand debonding may not eliminate the Y cracks at the ends of heavily prestressed girders. Therefore, two alternative debonding strategies were used for the 137 cm deep girders to eliminate the cracks. In the first alternate design, 38% percent of strands were debonded in the normal anchorage zone. In the second alternate design, 62% of strands were debonded at the girder end, but all with a short debonded length of 20 cm. (8 in.). Patterns of strands in the 137 cm deep girders are shown in Fig. 3.

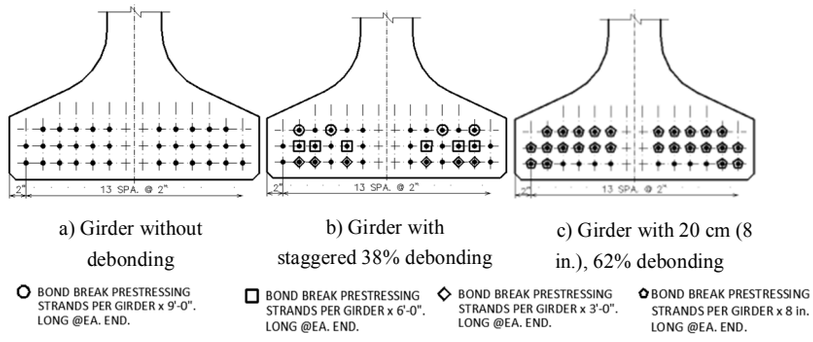

Fig. 3. Strand patterns for girder end with no debonding (a); for girder with 38% debonding (b) for girder with 62% debonding (c).

The most significant improvement in reduction of concrete tension strains was due to 62% debonding over 20 cm for Y cracking at the location of the third stirrup (VW2) from the end.

3 Analytical Simulations of Anchorage Zones

The results from the instrumented girders were used to validate nonlinear finite element analysis (FEA) models built to investigate various strand debonding amounts and patterns. This section presents the details of the FEA techniques.

Finite element simulations were executed using the commercial finite element software, Abaqus version 12.6 [8]. Models consisted of a nonlinear concrete end zone, a linear concrete region over the mid-span of the girder, and reinforcing steel bars. Since the goal was to control end zone cracking, it was unnecessary to model the full length of girder with nonlinear material properties as nonlinear computations can be computationally demanding. Based on St. Venant's principle, the stresses and strains are anticipated to have a linear distribution over the girder depth after a distance at least equal to the beam depth away from the anchorage region [9]. In addition, there were no cracks observed in actual girders after a length equal to twice the girder depth from the end. The length of the nonlinear concrete region was, therefore, restricted to twice the girder depth.

The size of the models was further decreased by modelling only a quarter of the full girders, utilizing symmetry in geometry and forces about the center plane of girder cross-section and about the middle plane of girder span. Prestress was applied as surface stresses around surfaces representing strand locations. A sample girder model is shown in Fig. 4. The shaded region is the end where non-linear modelling and small finite element size were used.

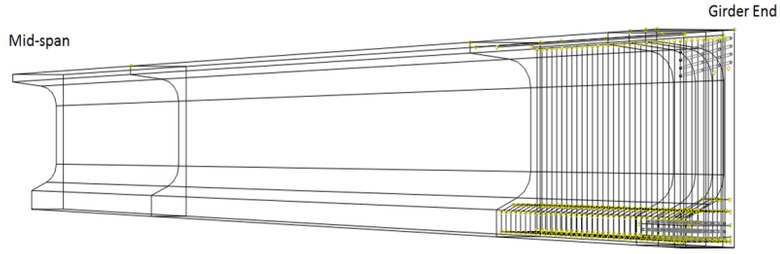

Fig. 4. Model of bonded 54W girder in Abaqus.

Up to the cracking strength of concrete, concrete theoretically behaves linearly and using linear FEA is sufficient and efficient. However, after cracking, stresses in concrete are redistributed and transferred to reinforcing steel crossing cracks through tension stiffening [10]. Tension stiffening of concrete was included in the models to capture the likelihood, approximate locations and severity of cracking, as well as stress changes in reinforcing bars upon cracking.

3.1 Compression Properties of Concrete

Concrete can be simulated using three different constitutive models in Abaqus: "the Concrete Damaged Plasticity", "the Smeared Cracking", and "the Brittle Cracking" models. The Concrete Damaged Plasticity model, based on the work of Lubliner et al. [11] and Lee [12], was selected. The strength of the concrete right before de-tensioning, as determined through cylinder tests, was used in the models. Material model for the linear stress range, i.e. before cracking, followed concrete linearity described in AASHTO LRFD Bridge Design Specifications 5.4.2.4 and 5.4.2.5 [7] as shown in Equation 1 (in MPa) and dependent on only an aggregate factor, the unit weight (kg/m^3) and the strength of concrete (MPa). The response of concrete was assumed to remain linear up to 40% of the concrete design strength. Material models for the nonlinear stress range followed concrete nonlinearity described in FIB 2010 Model Code [13] 5.1.8.1 as shown in Equation 2. The parameter definitions can be found in the Model Code text.

$$E_C = 0.043 K_1 {w_C}^{1.5} \sqrt{f'_C} \qquad \text{Equation 1}$$

$$\frac{\sigma_c}{f_{cm}} = -\left(\frac{k*\eta-\eta^2}{1+(k-2)*\eta}\right) \qquad for \;\; |\varepsilon| < \; |\varepsilon_{clim}| \qquad \text{Equation 2}$$

The descending part of the FIB 2010 Model Code compressive stress-strain curve is an envelope of all possible stress-strain relations of concrete, which

softens by micro-cracks, since the actual shape can depend on load redistribution, member geometry or specimen, and boundary conditions.

3.2 Tensile Properties of Concrete

Up to cracking, concrete tension stresses were assumed to be linearly proportional to strains. The modulus of elasticity, and poisson's ratio are the same as used for concrete in compression. The cracking strength, f_r (MPa), is taken as the limit for the elastic linear region as calculated by AASHTO LRFD Bridge Design Specifications C5.4.2.7 [7] as a function of f'c (MPa) and shown by Equation 3.

$$f_r = 0.7\lambda\sqrt{f_C'} \qquad \text{Equation 3}$$

Inelastic concrete tensile behaviour can be simulated based on concrete strain, crack opening, or fracture energy. This study used the relationship between crack opening and fracture energy to avoid results sensitive to mesh size. Mesh refinement does not always improve convergence in analyses with cracking, as mesh refinement leads to narrower crack bands [14]. Convergence problems can be solved without increasing the computation cost by defining reinforcing bars in concrete, which redistributes cracks with enough tension stiffening or by using Hillerborg's [15] fracture energy proposal. Hillerborg represents the energy required to open a unit area of crack, G_F , as a material parameter for brittle cracking. This approach expresses the brittle behavior by a stress-displacement response rather than a stress-strain response. Crack opening does not depend on the specimen's length and therefore, this approach applies to concrete of any shape. The fracture energy (N/m) was calculated per FIB 2010 Model Code [13] 5.1.5.2 as shown in Equation 4 where f_{cm} is mean compressive strength (MPa). The constitutive relationship of concrete in tension was defined as in section 5.1.8.2 of the FIB 2010 Model Code [13] using crack opening and fracture energy as given in Equation 5a and 5b.

$$G_F = 73 * f_{cm}^{0.18} \qquad in\ \frac{N}{m} \qquad \text{Equation 4}$$

$$\sigma_{ct} = f_{ctm} * \left(1.0 - 0.8 * \frac{w}{w_l}\right) \quad for\ w \le w_l \qquad \text{Equation 5a}$$

$$\sigma_{ct} = f_{ctm} * \left(0.25 - 0.05 * \frac{w}{w_l}\right) \quad for\ w_l < w \le w_c \qquad \text{Equation 5b}$$

In equations 5a and 5b, σ_{ct} is the tensile stress in MPa, f_{ctm} is the mean tensile strength of concrete in MPa, w is crack openning, w_l is crack openning when σ_c is equal to $0.2*f_{ctm}=G_F/f_{ctm}$, w_c is crack openning σ_c is equal to $0 = 5*G_F/ f_{ctm}$.

3.3 Properties of Reinforcing Steel

The analysis of girders showed that reinforcing bars in the end zones had stresses significantly below the yield strength. Therefore, reinforcing bars were modelled as linear elastic. The modulus of elasticity and poisson's ratio were taken as 200GPa (29000 ksi) and 0.3, respectively based on AASHTO LRFD BDS [7].

3.4 Strand Properties

Bond between concrete and strands can be modelled using springs, friction or cohesion to represent mechanical interlock, friction and adhesion [16]. For computational efficiency, the strands were excluded from the models and the bond stresses were directly applied to concrete where the surface of each strand would be located. Bond stresses were measured for the 183 cm girder by strain gages on strands along the transfer length and idealized as a constrant stress of 10.3 GPa (1500 ksi) between 0 cm (0 in.) and 20 cm (8 in.), 4.8 GPa (700 psi) between 20 cm (8 in.) and 51 cm (20 in.), and 0.24 GPa (35 psi) between 51 cm (20 in.) and 91 cm (36 in.) from the girder end.

4 Comparison of Experimental and Analytical Results

Concrete strains obtained through vibrating wire gauges and obtained through FEA were compared to evaluate the accuracy of the model input and modeling techniques. Fig. 5 is a comparison of strains from test and predictions from the FEA for 137 cm and 183 cm girders after all strand were cut. VW gage numbers on Fig. 5 refer to the numbers and locations given in Section 2. Girder Instrumentation Results of this paper. Gage numbers refer to gages at the same locations for the same girders. This figure can, therefore, also be used to compare strains in girders with and without debonding.

In general, FEA had good correlation with test results for large strains. For smaller strains (smaller than the cracking strain), the difference between FEA and test results was larger. This difference can be due to the sensitivity of the gages (+/- 15 microstrains), and the assumption of homogeneity of concrete in FEA. FEA was successful in predicting the locations of cracks, as indicated by high strains similar to those obtained from testing.

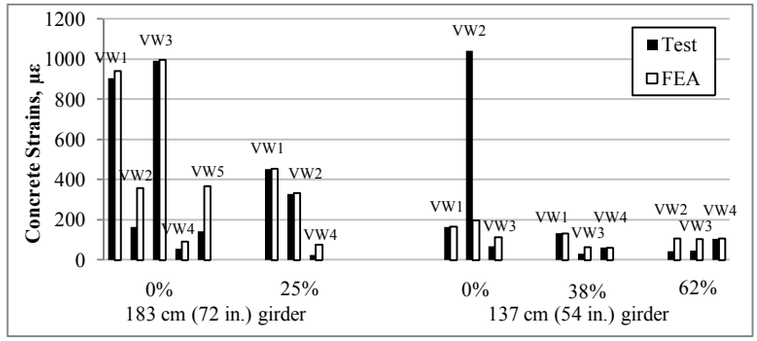

Fig. 5. Concrete strain comparison for 72W (left) and 54W girders (right) tested.

5 Debonding Ratios Required to Control Cracking

FEA was used to study the impact of varying levels of prestressing and debonding on end zone strains in a wide variety of girder configurations. Table 2 shows resultant strains in horizontal and Y cracking regions for varying ratios of debonding and number of strands. These girders represent cases where strains are small (smaller than 160 με), expected to have no cracking or very minor cracking.

		72W Girder		54W Girders	
Number of Strands	Strand Debonding- %	Max. Horizontal Strain- με	Max. Y crack Strain- με	Max. Horizontal Strain- με	Max. Y crack Strain- με
48	50	135	151	-	-
46	48	151	157	-	-
44	45	150	142	-	-
42	43	156	100	145	125
40	40	154	123	129	130
38	42	132	130	119	135
36	39	133	142	130	140
34	29	156	143	152	144
32	31	142	102	131	94
30	33	133	104	133	90
28	29	140	135	142	121

Table 2. Cracking strains for varying debonding ratios and number of strands.

6 Summary and Conclusions

This paper investigated the impact of debonding on pretensioned girder end zone cracking, particularly on cracks that can deteriorate girder durability. Two debonding methods were investigated: 1) debonding strands over a medium distance from the ends in the normal anchorage zone, and 2) debonding strands over a very short distance from the girder end. Five deep and heavily pretensioned bridge girders were instrumented during detensioning to provide a basis for evaluating analytical modelling. These girders included control girders with no debonding, and girders with various ratios of debonded strands. Instrumentation results showed that 25% percent debonding decreased horizontal web cracking and Y cracking concrete strains by 54% and 91%, respectively but cracking was not eliminated in a 183 cm deep girder. For 137 cm deep girders, debonding beyond 25% reduced all strains that would lead to Y cracking to a level below the cracking limit. FEA of girders was the used to extend the empirical study to a wider range of prestress levels and debonding ratios. Nonlinear material properties increased the computational demand but ensured proper representation of cracking in models.

Results of FEA and tests had acceptable correlation. The ratio of debonding that can eliminate both horizontal web cracks and Y cracks was determined to range between 29% and 50% for 137 cm and 183 cm deep girders with the number of strands used varying between 34 and 48 respectively. Debonding is an efficient method for controlling or eliminating Y cracks at the ends of girders. The number or percentage of strands to be debonded changes with the total number of strands in the beam.

Acknowledgments This research was conducted with support from Wisconsin Highway Research Program (WHRP). The authors would like to acknowledge WHRP for financial support and the members of the Project Oversight Committee for technical guidance. The conclusions in this paper are those of the authors and do not necessarily reflect the views of WHRP. The authors would also like to thank Spancrete and County Material for accommodating the research team at their plants.

References

1. Arab A., Badie S.S., Manzari M.T., Khaleghi B., Seguirant S.J., Chapman D. Analytical Investigation and Monitoring of End-zone Reinforcement of the Alaskan Way Viaduct Super Girders. Precast/Prestressed Concrete Institute Journal, Spring 2014, Vol. 59, No. 2. pp. 109-128.

2. Okumus, P., and Oliva, M. G., Evaluation of Crack Control Methods for End Zone Cracking in Prestressed Concrete Bridge Girders. PCI Journal, Spring 2013, Vol. 58, No. 2, pp. 91-105.

3. Okumus, P., Oliva, M. G., and Becker, S., Nonlinear Finite Element Modeling of Cracking at Ends of Pretensioned Bridge Girders. Engineering Structures, July 2012, Vol. 40, pp. 267-275.

4. Okumus, P., and Oliva, M. G., Strand Debonding for Pretensioned Bridge Girders to Control End Cracks. ACI Structural Journal, Jan.-Feb. 2014, Vol. 111, No. 1, pp. 201-210.

5. Okumus P., Kizilarslan E., Oliva M.G., Yang C., Anchorage Zone Cracking Evaluation in De-bonded Deep Bulb-Tee Bridge Girders. Proceedings of the PCI Convention and the National Bridge Conference at Nashville, Tennessee on March 2-5, 2016, paper ID: 34, pp. 12.

6. Kizilarslan, E., De-bonding Strands as an Anchorage Zone Crack Control Method For Pre-tensioned Concrete Bulb-Tee Bridge Girders Using Nonlinear Finite Element Analysis. MS Thesis, Madison, WI: University of Wisconsin-Madison, 2016.

7. American Association of State Highway and Transportation Officials (AASHTO), AASHTO LRFD Bridge Design Specifications, U.S. Units, 7th Edition, with 2015 Interim Revisions, Washington, DC, 2014, pp. 1960.

8. Dassault Systemes Simulia Corporation. RI, USA: Dassault Systemes, 2012.

9. R. A. Toupin, Saint-Venant and Matter of Principle. Trans. N.Y. Acad. of Science, series 11, December 1965, Vol. 28, No. 2, pp. 223.

10. Floegl H., Mang H. A., Tension Stiffening Concept Based on Bond Slip. American Society of Civil Engineers (ASCE) 1982, Vol. 108, Issue 12, pp. 2681-2701

11. Lubliner, J., Oliver, J., Oller S., Oñate E., A plastic-Damage Model for Concrete. International Journal of Solids and Structures. 1989, Vol. 25, No. 3, pp. 299-326.

12. Lee, J., and Fenves, G. L., Plastic-Damage Model for Cyclic Loading of Concrete Structures. Journal of Engineering Mechanics, August 1998, Vol. 124, No. 8. pp. 892-900.

13. Federation Internationale du Beton. Model Code 2010 – First Complete Draft., April 2010.

14. Dassult Systemes Simulia Corporation.RI, USA:Dassault Systemes, 2009. Abaqus Theory Manual (6.9). Available at:

http://www.egr.msu.edu/software/abaqus/Documentation/docs/v6.7/books/usb/default.htm?startat=pt05ch18s05abm36.html

15. Hillerborg,A., Modeer, M., Peterson P.E., Analysis of Crack Formation and Crack Growth in Concrete By Means of Fracture Mechanism and Finite Elements.Cement and Concrete Research at Lund Institute of Technology (Pergamon Press, Inc.), August 24, 1976, Vol. 6, pp. 773-782.

16. Okumus, P., Nonlinear Analysis of Pretensioned Bridge Girder Ends To Understand and Control Cracking At Prestress Release. PhD Ed. Madison, WI: University of Wisconsin-Madison, 2012.